Technical Assessment
GSI-193, BWR ECCS Suction Concerns

Geometrical and Operational Characteristics Affecting the Ingress of Non-condensable Gases in the BWR ECCS System During a HELB Accident

Prepared by:
Alexander Velázquez-Lozada
10/25/2005

Revised by:
Alexander Velazquez-Lozada
8/31/2010

CONTENT

FIGURES

Page

TABLES

Page

EXECUTIVE SUMMARY

This report is part of the technical assessment required per Task Action Plan to solve the Generic Safety Issue (GSI) 193, "BWR ECCS Suction Concern." This reports presents the effects that the suppression pool geometry and ECCS response has in the potential of gas ingress into the ECCS system during a high energy line break(HELB)

GEOMETRICAL

NON-CONDENSABLE GAS SOURCES

The principal source of non-condensable gases that may enter into the ECCS system is the gas from the drywell. The amount of non-condensable dissolved in the suppression pool, represent no more than 2% of void fraction.

MECHANISM THAT MAY CAUSE GAS INGRESS

The blowdown force and the ECCS suction force have been identified as the two driven forces of the suppression pool dynamics during HELB. The blow down force generates four potential mechanisms of gas ingress: (1) the liquid-gas jet, (2) pool temperature rise, (3) pressure drop and (4) turbulence. The ECCS suction has the potential to drawn gas from the suppression pool and to cause a pressure drop at the ECCS strainer, causing gas to come out of the water. The column of water of the partially submerged downcomer generates an initial liquid jet, which kinetic energy (KE) has been identified as a major force to break bubbles and to generate a circular motion (vortex) in the suppression pool. Among the two containment with vertical downcomers analyzed in this report, the initial liquid injection at Mark-II has a KE three times higher than Mark-I.

DOWNCOMERS

The alignment between downcomers and strainers in Mark-I containment has been identified as a significant geometrical characteristic that may cause gas ingress into the ECCS during the initial blowdown. Although the strainers in Mark-II containment are not aligned in a direct path, the location of the strainer exposes it to the bubbles, which are rising to the surface. The distance between the downcomers and strainers in Mark-III is large compare to Mark-I and II. For that reason the potential of gas ingress during the initial blowdown is low.

OPERATIONAL

ECCS OPERATION

The operation of the ECCS with normal AC power and without failure of any ECCS component is the operational status that may cause the greatest ingress of gas into the system. This status is the fastest to start the flow of suppression pool water into the ECCS (immediately upon the start of a LOCA event), and it is characterized by the highest volumetric flow.

RING HEADER

The presence of a ring header deters gas ingress through the two core spray (CS) pump strainers; however, it exacerbates gas ingress through the eight low-pressure coolant injection (LPCI) pump strainers.

1. INTRODUCTION

This report presents the first technical assessment outlined in the Task Action Plan [Ref. 1] for resolving Generic Safety Issue (GSI) 193, "BWR ECCS Suction Concerns."

The purpose of this assessment is to identify the geometrical characteristics and operational conditions that may cause non-condensable gas to enter the emergency core cooling system (ECCS) suction piping as a result of a break of a high energy line inside a boiling water reactor (BWR) containment. Non-condensable gas ingress into a pump suction pipe might degrade the capability of the ECCS pump to mitigate the accident. All ECCS pumps are safety-related equipment and, as such, must be operable to ensure core cooling, as required by Title 10, Section 50.46(b)(5), of the *Code of Federal Regulations* (10 CFR 50.46) [Ref. 2].

This assessment evaluated two sources of non-condensable gas with the potential to enter into the ECCS system suction piping as a result of an accident blow down. The two sources are described in Section 3 of this report. The mechanisms that induce non-condensable gases, as well as the geometrical and operational characteristics that enhance gas ingress in the ECCS system, are discussed in the subsequent sections.

Two postulated accidents with the potential to cause non-condensable gas ingress into the ECCS system, are a liquid line break loss-of-coolant accident (LOCA) and a steam line break accident (MSLBA). The relative severity of these accidents depends of the plant design. One of the design basis accidents (DBA) is defined as a double-ended guillotine full offset rupture in a pipe of the coolant-system. The LOCA has been selected in this report for the preliminary technical assessment. The next section describes the classification of small, medium, and large break LOCAs.

2. LOSS OF COOLANT ACCIDENT

According to a document from the Office of the Secretary of the Commission (SECY-04-0060) [Ref. 3], the LOCA events are classified in six categories. As can be observed in Table 1, the categories are defined over a range of break flow rates.

Table 1: LOCA Category Definitions.

LOCA Category	Flow Rate			LOCA Classification
	gpm	m^3/s	ft^3/s	
1	> 100	0.00631	0.22	SB
2	> 1,500	0.09465	3.3	MB
3	> 5,000	0.3155	11.1	LB
4	> 25,000	1.5775	55.7	LB a
5	> 100,000	6.31	222.8	LB b
6	> 500,000	31.55	1114.2	LB c

Legend:
SB = small break
MD = medium break
LB = large Break

The pipe break of the recirculation line is considered as a precursor of a large-break LOCA. As can be observed in Figure-1, this break occurs between the recirculation pump and the outlet nozzle of the reactor vessel.

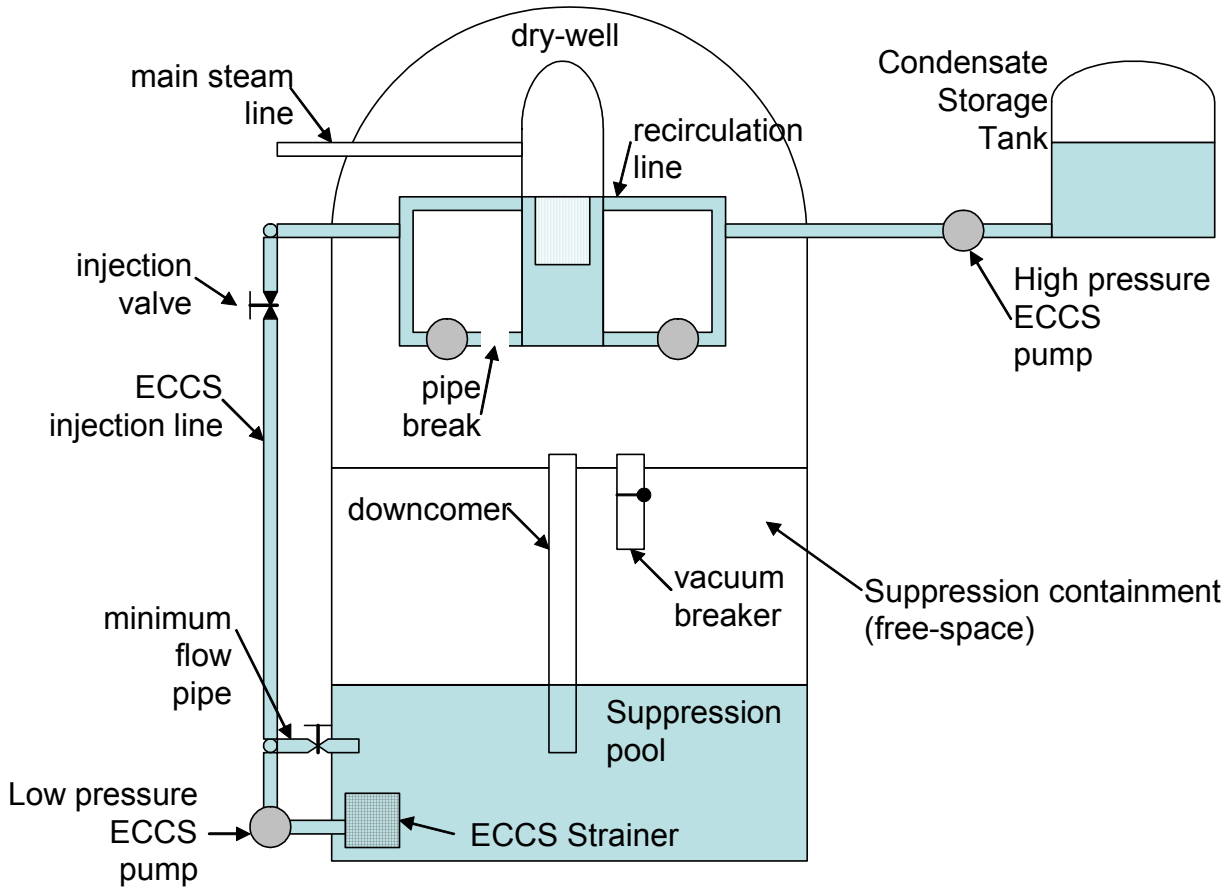

Figure 1. Simplified Typical BWR Configuration

When a recirculation line breaks occurs, a significant amount of water flashes to steam as it exits the break. The expanding volume of steam in the drywell displaces the non-condensable gas, liquid, and vapor from the drywell into the suppression pool via the down comers. The non-condensable gas present in the dry-well is one of the sources of gas with potential to enter into the low-pressure ECCS during an event. This and other sources of gas, that may enter into the low-pressure ECCS suction piping, are explained in more detail in the next section.

The high pressure system is not included in this preliminary analysis.

3. SOURCES OF NON-CONDENSABLE GASES

The sources of non-condensable gases involve the air in the dry-well volume and the air dissolved in the suppression pool water. The amount of air in the dry-well depends of its size and conditions during normal operation. The amount of gas dissolved in the suppression pool water depends of the solubility of the non-condensable gases in the water.

The dry-well volume, and operational (i.e., pressure and temperature) conditions, differ from plant to plant. Table 2 summarizes some general characteristics of a typical Mark-I, II, and III BWR NPP Containment.
of these three plants are representative of Mark-I, Mark-II, and Mark-III plants, respectively.

Table-2: General Characteristic of BWR NPPs

	Mark-I	Mark-II	Mark-III
i.			
Recirculation line			
Single pump flow,m^3/s(gpm)	2.85 (45200)	2.85 (45200)	2.05 (32500)
Water Temperature, ^{o}C (^{o}F)	288.3 (551)	288.4 (551.1)	289.44 (553)
Dry-well			
composition	Nitrogen	Nitrogen	Air
free volume, m^3 (ft^3)	4,142 (146,266)	6,897 (243,580)	6,688 (236,196)
*pressure, KPa (psia)	113.4 (16.45)	106.5 (15.45)	101.3 (14.7)
*temperature, ^{o}C (^{o}F)	65.5 (150)	65.5 (150)	62.7 (145)
design pressure, KPa (psia)	386 (56)	379 (55)	172 (25)
design temperature, ^{o}C (^{o}F)	171 (340)	171 (340)	165 (330)
Suppression containment			
free volume, m^3 (ft^3)	3114.8 (110000)	4181.5 (147670)	3629 (128160)
*water volume, m^3 (ft^3)	2453.7 (86652)	3359 (118655)	3622 (127934)
*pressure, KPa (psia)	113.4 (16.45)	106.5 (15.45)	101.3 (14.7)
*water temperature, ^{o}C (^{o}F)	37 (100)	35 (95)	37 (100)
design pressure, KPa (psia)	386.1 (56)	379.2 (55)	137.9 (20)
design temperature, ^{o}C (^{o}F)	171 (340)	171 (340)	85 (185)

The next sections present the calculations to estimate the total mass of non-condensable present in the dry-well and the dissolved gases in the suppression pool water.

3.1 Non-condensable gases in the dry-well

Assuming that the non-condensable gases in the dry-well behaves as ideal gases, we can use equation 1 [Ref. 7] to estimate the mass of gas in the dry-well of a typical Mark-I, Mark-II, and Mark-III plant.

$$PV = mRT$$ Equation-1

Where P = pressure (Pascal),
V = volume (m^3),
m = mass (Kg),
R = gas constant (J/Kg.K), and
T = temperature (Kelvin).

Solving for mass we get:

$$m = \frac{PV}{RT}$$

The gas constant for nitrogen, R = 296.77 (J/Kg.K), and the gas constant for air, R = 287.03 (J/Kg.K). Table-3 summarizes the results of the calculation for the amount of non-condensable gas present in the dry-well of the previous selected plants.

Table-3: Non-condensable mass in the dry-well, (kg)

Mark-I	Mark-II	Mark-III
4682.12	7305.01	7022.79

Other source of non-condensable gases is the gas dissolved in the suppression pool water, whish is discussed in the next section.

3.2 Dissolved gas in the suppression pool water

The solubility of gases in water, typically increase as pressure increase and decrease as temperatures increases. The solubility (mole ratio basis) of nitrogen and oxygen in water at 25 °C and 1 atm (101.3 kPa) are 0.000012 and 0.000023 respectively [Ref. 8]. Air is composed roughly of 75.47% nitrogen and 23.2 % oxygen by weight. We can deduct immediately that water exposed to an environment rich of nitrogen will have less non-condensable gases dissolved than water exposed to normal air.

The suppression pool water is typically very close to 25 °C and 1 atm (101.33 kPa). We can use the previous solubility values to estimate the initial amount of gas dissolved in the water. This estimation can be done for water exposed to air as the cover gas and water exposed to a nitrogen as the cover gas.

First, we convert the mole ratio to mass ratio using the molecular weight of the components (Table-4) and Equation 2. Having this value we can estimate the total mass of non-condensable gases dissolved in the supersession pool water.

Table 4: Molecular Weights of nitrogen, oxygen, and water

N2	O2	H2O
28	32	18

$$Mass\ Ratio_{\frac{solute}{solvent}} = \frac{MW(solute)}{MW(solvent)} \cdot (Molar\ Ratio_{\frac{solute}{solvent}}) \cdot (\%\ per\ weight_{\frac{solute}{solvent}}) \qquad \text{Equation-2}$$

For a nitrogen cover gas, the solubility values used are from the experiments published in "Atomnaya Energiya," in 1988, [Ref. 9]. The solubility of nitrogen for the specific suppression containment conditions of Mark-I and Mark-II (NPP) are calculated by interpolating between solubilities for different pressures and temperatures. Results of the interpolation are shown in Table

Table 5: Solubility (molar ratio) of nitrogen in water
for different pressures and temperatures

	Temperature (deg Celcius)			
Pressure Kpa)	(20	35	37	40
100	1.490E-05	1.183E-05	1.142E-05	1.080E-05
101.3	1.509E-05	1.199E-05	1.157E-05	1.095E-05
106.5	1.585E-05	1.263E-05	1.220E-05	1.156E-05
113.4	1.685E-05	1.349E-05	1.304E-05	1.237E-05
500	7.320E-05	6.150E-05	5.994E-05	5.760E-05

Table-6 summarizes the results for the calculation of the total mass of non-condensable gases dissolved in the suppression pool water.

Table 6: Total mass of non-condensable gases present in selected BWR dry-wells

	Mark-I	Mark-II	Mark-III
percent per weight of N2 in wet-well	100.00%	100.00%	75.47%
percent per weight of O2 in wet-well	0.00%	0.00%	23.20%
water volume, m^3	2453.7	3359	3622
water temperature, deg C	37	35	37
pressure, Kpa	113.4	106.5	101.3
water density, Kg/m^3	992.2	993.2	992.2
mass of water, Kg	2434561.14	3336158.8	3593748.4
solubility (mol ratio) N_2/H_2O	1.30406E-05	1.26322E-05	1.20E-05
solubility (mol ratio) O_2/H_2O	n/a	n/a	2.30E-05
initial mass ratio of N_2/H_2O	2.02854E-05	1.96501E-05	1.41E-05
initial mass ratio of O_2/H_2O	n/a	n/a	9.49E-06
total initial mass ratio of non-condensable gases	2.03E-05	1.97E-05	2.36E-05
total initial mass of non-condensable gases, Kg	49.39	65.56	84.72

Comparing Tables 3 and 6, the mass of non-condensable gases dissolved in the suppression pool is very small compared with the mass of non-condensable gases available to be injected into the suppression pool from the dry-well (Table-3) during a LOCA or S.B. accident. Although small, the contribution of the dissolved non-condensable gas in the pool to the overall non-condensable gas void fraction in the suppression pool is considered in this preliminary analysis. An estimate of maximum potential void fraction (MPVF) due to non-condensable gases in the suppression pool can be calculated. The MPVF for the conditions presented in Table 2, can be calculated assuming all the dissolved gas come out of solution and that all gases behave as ideal gases. Table-7 summarizes the results for the MPVF calculated for typical BWR NPPs.

.

Table 7: Maximum potential void fraction for Mark-I, II, and III.

	Mark-I	Mark-II	Mark-III
potential volume of non-condensabel gases	40.25	56.53	74.51
maximum potential void fraction	1.61%	1.66%	2.02%

Previous analysis [Ref. 9] demonstrated, for water exposed to air at atmospheric pressure, that an increase from 20 ^oC to 90 ^oC causes a release of 1.463 cubic centimeter of air per 100 grams of water. This represent roughly 1.36% void fraction. In the calculations on Ref. 9 the pressure was held constant. A pressure increase would decrease the release of the gas from the solution.

The next section discusses the mechanisms that might cause non-condensable gases to enter the ECCS pump suction lines via the suppression pool.

4. POTENTIAL MECHANISMS OF GAS INGRESS

There are several mechanisms that might have the potential to induce gas ingress into the ECCS system during a postulated LOCA or S.B. accident. The mechanisms that might combine to potentially cause non-condensable gases from the dry-well to enter the ECCS suction piping are gas-liquid jetting, pool turbulence, and ECCS pump suction flow. The mechanisms that might combine to cause the dissolved gases to enter the ECCS system are the gas coming out of the solution from suppression-pool water due to pool temperature rise and localized pressure drops. ("Gas-evolution" is another term used to describe the phenomena of gases coming out of the a solution.)

Figure-2 illustrates the different mechanisms that can potentially induce gas ingress into the ECCS system through the strainer. As can be observed from the figure, a LOCA results in two significant time-dependant forces that effect the transport of non-condensable gases within the suppression pool. These are (1) the differential pressure between the dry-well and the wet-well that creates a blow-down force on the non-condensable gases, expelling the gas from the dry-well into the suppression pool and, (2) the suction-force within the ECCS pump suction lines due to operation of the pumps.

The timing of these forces is important to determine the extent to which non-condensable may enter the ECCS pump suction lines. The start-up sequence of the ECCS system (i.e., pumps start) depends of the plant design and operational status of the plant at the time of the pipe break.

The initial blow-down of non-condensable gas through the downcomers creates a strong jetting action within the suppression pool water. The distance a non-condensable gas jet extends from the bottom of the downcomer will depend of the size of the pipe break, the available vent area, the orientation of the down-comer and the elapsed time from the break. Also, the ECCS pipes that draw suction from the suppression pool water come equipped with suction strainers. The alignment between a down-comer and a strainer can effect the extent to which there may be direct jetting of non-condensable gases into the suction strainer. The strong jetting action induce a circular motion; and also the break-up of gas into smaller bubbles. The circulation can be strong enough to keep smaller bubbles in the suppression pool for an specific period of time.

The jet injected into the suppression pool is composed by non-condensable gases, hot water, and steam. The injection of hot steam into the suppression pool cause the temperature of the water to increase. On the other hand, the injection of non-condensable gases make the pressure of the suppression containment to increase. This two mechanism compete in the suppression pool to release or suppress the release of gas from the suppression pool water. Any released gas will mix with dry-well gas in the turbulent circulating motion induced by the blow-down force.

The gases mixed in the suppression pool water could be drawn into the ECCS system if the suction force, cause by the operating ECCS pumps, is strong enough. The suction force (i.e., flow velocity) are time dependant and depend on the instantaneous pump flow rate and the size and configuration of the ECCS pump suction piping. This suction force causes a time-

dependant local pressure drop at the ECCS strainer. This pressure drop could cause additional dissolved non-condensable gas (i.e., bubbles) within the pool to come out of solution within the strainer and be drawn into the ECCS system suction piping. The pressure drop will depend of the characteristics of the strainer and the suction flow velocity at the strainer.

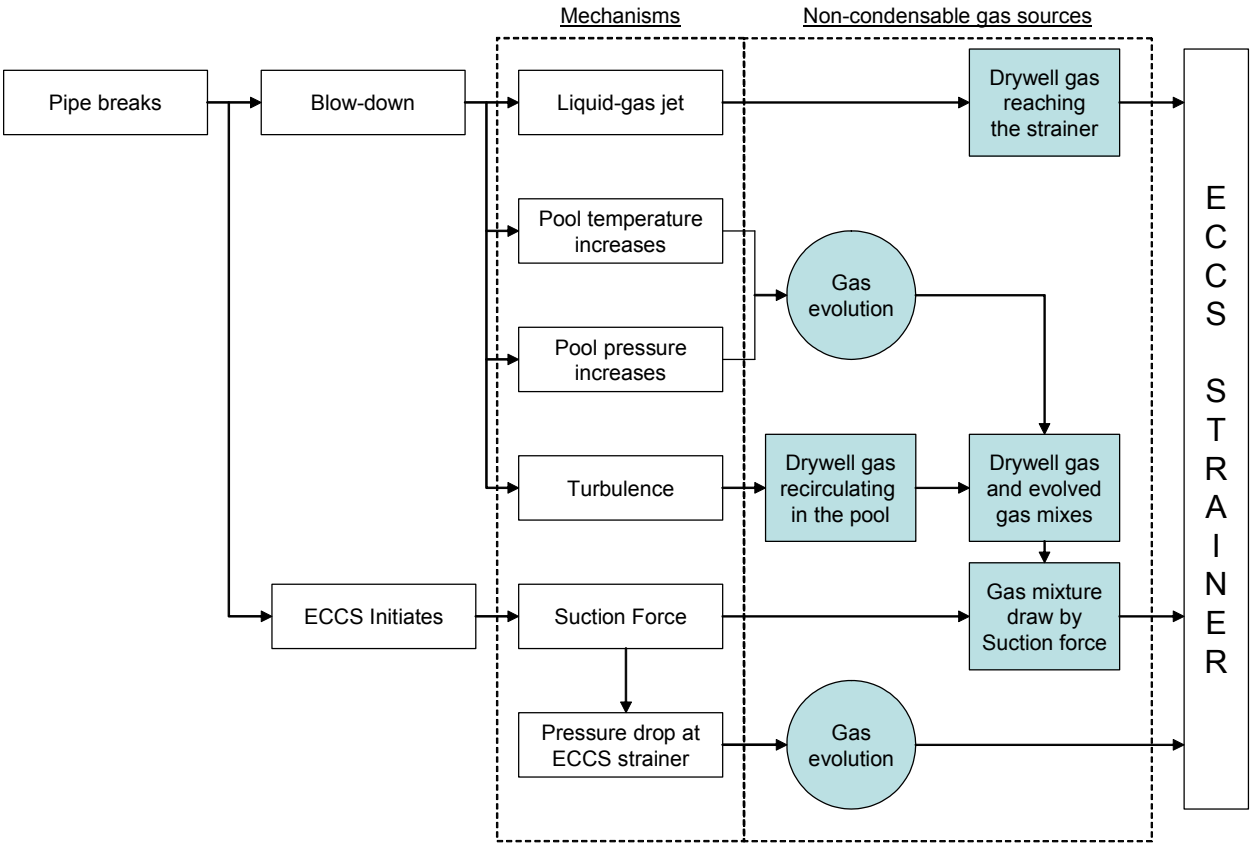

Figure 2: Potential Mechanisms that cause gas ingress into the ECCS system

The next sections describe in more detail the geometrical characteristics and operational conditions that impact the liquid-gas jetting effect and the ECCS suction force.

5. GAS LIQUID JET

5.1 Velocity of the liquid-gas jet

The time-dependant penetration and duration of the liquid-gas jet depends of the size of the pipe break, the available vent area of the down-comers and the time following the break (i.e., the blowdown rate and non-condensable gas remaining in the dry-well). As mentioned in

previous sections, the steam generated during a pipe-breaks forces the gas from the dry-well to the suppression pool. Although, not all of the reactor coolant flashes to steam during a LOCA , the specific volume of steam at low pressure (and low temperature) is several orders of magnitude higher than the specific volume of water at high pressure (and high temperature). For that reason, the volumetric flow of steam coming from the pipe-break will rapidly force (i.e., displace) the gas into the suppression pool.

The volumetric rate of steam flow into the dry-well can be estimated based on an iso-enthalpic expansion of the hot reactor coolant water. The following calculations provide a first order approximation without consideration of the effects of geometry on the velocity of the liquid-gas jet and therefor provide an estimate of the velocity of the down-comer jet in a BWR constrainment.

It is assumed that the reactor coolant temperature is very close to the saturation temperature of the reactor at normal operating pressure. It is also assumed that the pressurized reactor coolant expands very rapidly and exceeds the dry-well normal operating pressure and rapidly exceeds the additional (i.e., higher) pressure head of the water column in the down-comer. At this pressure, the standing water column in the down-comer will be fully displaced into the pool.

The down-comer submergence is different in the three selected plants. As can be observed in Figure-3, the submergence of the down-comers at Mark-I and Mark-II are 1.32 meter (4.4-ft) and 3.73 meter (12.25 ft.) respectively. Mark-III containment has the vents distributed in the rows at different levels. It is expected for a large brake LOCA that the blow-down will happen through the three rows of vents in a Mark-III containment.

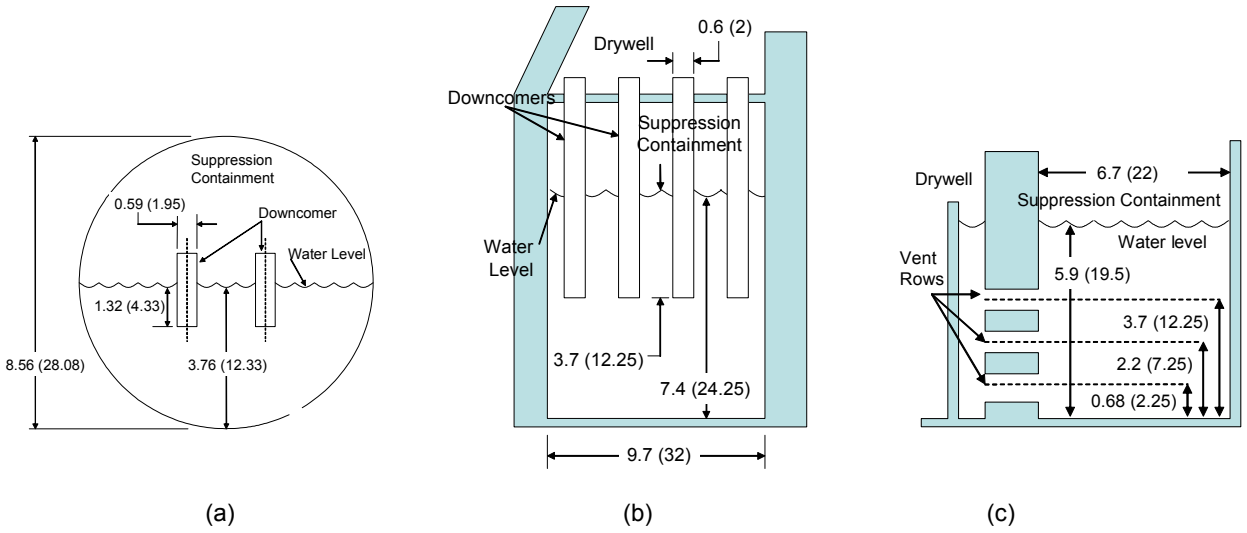

Figure 3: Cross section and dimensions of a typical
(a) Mark-I, (b) Mark-II, and (c) Mark-III suppression containment

Table 8, summarizes the results for the estimated pressure at which the saturated liquid will expand iso-enthalpically.

Table 8: Estimated Pressure at which the steam will expand

	Mark-I	Mark-II	Mark-III
donwcomer submergence, m (ft)	1.32 (4.33)	3.73 (12.25)	5.27 (17.25)*
Downcomer pressure-head, kPa	12.95	36.59	51.70
Expansion pressure, kPa	126.35	143.09	153.00

* depth of the third row vents

The first step is to find the conditions of the steam after the iso-enthalpic expansion. The enthalpy of the coolant water is for saturated water. Assuming constant enthalpy at normal operating dry-well pressure, the steam conditions after the expansion may be estimated. The expansion of saturated water produces a mixture of liquid and vapor. The fraction of steam in the mixture is calculated using equation-3. And the specific volume of the mixture (vx) is calculate with equation-4. Table-9 summarizes the results for the estimated specif volume of the mixture at the dry-well pressure.

$$x = \frac{hf_1 - hg_2}{hf_2 - hg_2} \qquad \text{Equation-3}$$

$$vx_2 = vf_2 + x\left(vg_2 - vf_2\right) \qquad \text{Equation-4}$$

Where:
hf_1 = entropy of fluid at coolant temperature
hf_2 = entropy of fluid at dry-well pressure
hg_2 = entropy of steam at dry-well pressure

and
vx_2 = specific volume of mixture at dry-well pressure
vf_2 = specific volume of fluid at dry-well pressure
vg_2 = specific volume of steam at dry-well pressure

Table 9. Thermodynamics properties of steam after iso-enthalpic expansion

				specific volume cm^3/g			enthalpy KJ/(kg*K)		
	Press. (KPa)	Temp.(°C)	x	vf	vx	vg	hf	hx	hg
	Mark-I								
1	-	290.0	-	1.37	-	25.54	1289.10	-	2766.20
2	126.3	-	0.377	1.05	566.42	1499.90	443.62	1289.10	2685.04
	Mark-III								
1	-	290.0	-	1.37	-	-	1289.10	-	2766.20
2	143.1	-	0.372	1.04	590.04	1586.25	460.20	1289.10	2691.10
	Mark-III								
1	-	290.0	-	1.37	-	-	1289.10	-	2766.20
2	153.0	-	0.371	1.04	621.10	1672.55	461.92	1289.10	2691.79

Using the values from Table 8 we calculated the liquid to mixture expansion ratio (LMER). These values are tabulated in Table 10.

Table 10: Summary of vapor to mixture expansion ratio calculations

	Mark-I	Mark-II	Mark-III
specific volume of saturated liquid at recirculation temperature, cm^3/g	1.37	1.37	1.37
Quality of steam at dry-well pressure, %	0.38	0.37	0.37
specific volume of saturated steam at estimated dry-well pressure, cm^3/g	566.42	590.04	621.10
vapor to mixture expansion ratio (LMER)	414.78	432.07	454.82

Using the estimated liquid-to-mixture expansion ratio (LMER) the rate of volumetric flow of expanded mixture pushing the non-condensable gas in the dry-well into the suppression pool can be calculated for various LOCA break sizes with the following formula:

$$V_{expanded} = LMER \times V_{recircularion\ line} \quad \text{Equation-5}$$

Where:

$V_{expanded}$ = Volumetric flow of the expanded mixture, and
$V_{recircualtion\ line}$ = Volumetric flow of saturated water inside the recirculation line.

From Table-2, we know that volumetric-flows in a single recirculation line are 2.85 m^3/s for

Mark-I and Mark-II; and 2.08 m^3/s for Mark-III. Table-11 summarizes the volumetric flow for different sizes of pipe breaks and for the specific DBA for a recirculation line break in the selected plants.

Table 11: Expanded volumetric flow of the mixture for different pipe breaks assuming iso-enthalpic expansion at dry-well conditions (m^3/s)

LOCA Category	coolant volumetric flow (m^3/s)	Mark-I .	Mark-II	Mark-III
1	0.00631	2.62	2.73	2.87
2	0.09465	39.26	40.90	43.05
3	0.3155	130.86	136.32	143.49
4	1.5775	654.32	681.59	717.47
5	6.31	2617.26	2726.36	2869.89
6	31.55	13086.30	13631.82	14349.46
Plant Specific DBA				
	2.85	1182.12	1231.40	N/A
	2.05	N/A	N/A	932.37

As can be observed on Table-1, no significant pressure-difference exist between the dry-well and the wet-well during normal operation. Assuming that there are no frictional losses during the blow-down, the initial velocity of the liquid-gas jet for each one of the selected plants can be estimated. The velocity is calculated by dividing the expanded volumetric flow rate by the total available down-comer cross-sectional area. Table-12 summarizes the estimated initial velocity of liquid-gas jets entering the pool for the selected plants. The pressure and temperature in the dry-well and wet-well is expected to increase during the blow-down process, but for comparison purposes in this report they are assumed to remain constant.

Table 12: Estimated velocity of the liquid-jet for different size of pipe breaks (m/s)

		total vent area (m^2)				
LOCA Category	coolant volumetric flow (m^3/s)	Mark-I .	Mark-II .	Mark-III, .		
				3 rows	2 rows	1 row
		22.39	22.73	49.42	32.95	16.47
1	0.00631	0.12	0.12	0.06	0.09	0.17
2	0.09465	1.75	1.80	0.87	1.31	2.61
3	0.3155	5.84	6.00	2.90	4.35	8.71
4	1.5775	29.22	29.98	14.52	21.77	43.55
5	6.31	116.90	119.93	58.07	87.10	174.20
6	31.55	584.48	599.64	290.33	435.50	870.99
Plant Specific DBA						
	2.85	52.80	54.17	N/A	N/A	N/A
	2.05	N/A	N/A	18.86	28.30	56.59

From Table-12, the velocity of the jets of Mark-I and Mark-II are very similar.

The jet velocity for Mark-III is about half that of Mark-I and Mark-II for the three rows case. The potential for gas being forced into an ECCS pump suction strainer will depend of the orientation and proximity of the down-comer relative to the strainer. The down-comers of Mark-I and Mark-II are vertical and the down-comers of Mark-III are horizontal.
The potential for the jets passing into the strainers is discussed in the next section.
.

5.2 Potential reach of the liquid-gas jet

The potential for gas reaching the strainer depends of the proximity and orientation of the down-comers relative to the strainers. In Mark-I and Mark-II containment, the down-comers are align vertically; mean while in Mark-III containment, the down-comers are aligned horizontally.

When gas is injected in water through an orifice, it will tend to form a bubble that will detach when it reaches an specific volume. Equation-6 has been proposed by Davidson and Amick [Ref. 11, and 12] to estimate this volume. Although Equation-6 is commonly used for upward gas injection, it can be used to estimate the radius of the bubble formed for downward injection cases.

$$V_b = 1.138 \frac{\dot{V}_g^{\frac{6}{5}}}{g^{\frac{3}{5}}} \qquad \text{Equation-6}$$

Where:
V_b = bubble volume
V_g = volumetric gas flow rate
g = gravity acceleration

Gas injected into the pool at a high rate of mass flow leaves the orifice as a continuous jet rather than a series of large bubbles. Equation-7 has been proposed by Kutateladze and Styrikovich as a condition for the formation of a gas jet.

$$\frac{v_g \sqrt{\rho_g}}{\left[g\sigma\left(\rho_f - \rho_g\right)\right]^{\frac{1}{4}}} > 1.25\left[\frac{\sigma}{g\left(\rho_f - \rho_g\right)R_o^{\,2}}\right]^{\frac{1}{2}} \qquad \text{Equation-7}$$

Where:
v_g = gas velocity,
ρ_f = liquid density,
ρ_g = gas density,
σ = liquid-gas interfacial surface tension, and
R_o = orifice radius.

For an interfacial surface-tension of 0.07 N/m (air and water at standard conditions) and an average pipe radius 0.3 meters; the right-hand side of the equation-4 yield approximately 0.01. The left-hand-side of equation-4 yield numbers higher than 0.01 for all the estimated gas velocities of medium and large LOCAs summarized in Table 11. According to Kutateladze and Styrikovich condition the injection of gas in the suppression pool during the initial blow-down will be in the form of a jet. Is suggested that bubble formed in the jet regime are almost twice the orifice diameter [Ref. 11].

In order to estimate the distance of the bubble and/or gas-jet, from the bottom of the down-comer, it may be assumed that the diameter of biggest bubble formed at the end of the pipe will be twice the pipe diameter. The diameter of the down-comers in the three selected plants is about 0.6 meters. The estimated bubble size would be 1.2 meters in diameter. The potential for such a bubble reaching a strainer may be estimated based on the strainer location relative to the outlet of the nearest down-comer.

The analysis of Mark-I containment indicates that some strainers are located close to the vertical down-comer outlet which may enable bubbles to come in contact with a strainer.

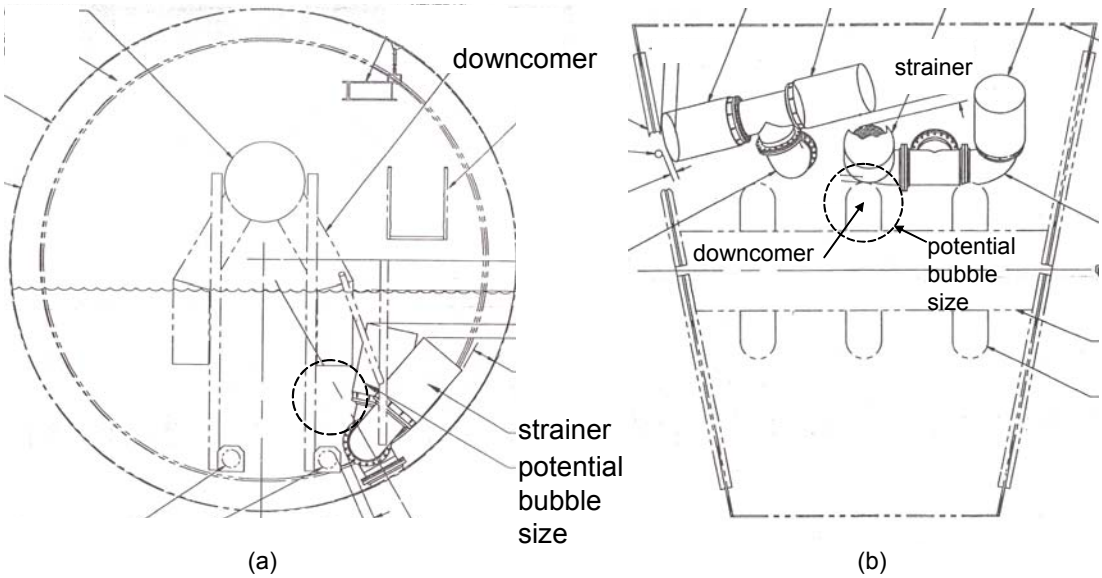

Figure 4: (a) Cross-sectional view and (b) top view of the suppression containment of typical Mark -I NPP.

Figure 4 shows the potential volume of the initial bubble relative to the location fo a strainer. which increase the possibility of gas ingress in the ECCS system. Experimental data would be necessary to reduce the uncertainty associated with the proximity of a gas bubble to a strainer.

This bubble/jet is formed assuming that the column of water inside of the down-comer has already been displaced. In the real scenario the down-comer are partially filled with water at the beginning of the blow-down process. The displacement of this column of water at the velocities estimated in previous sections, will induce a recirculating motion (Figure-5) and shear forces that break bubbles into smaller sizes. This recirculating motion might have the effect of keeping the smallest bubbles in the flow field near the strainer for a period of time after the blow-down ends.

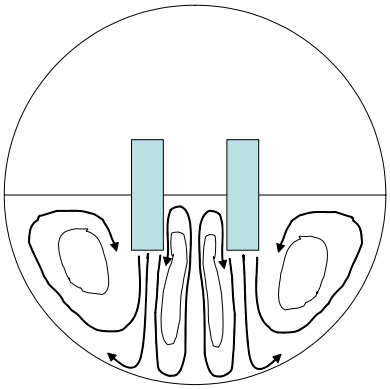

Figure 5: Potential vortex motion in Mark-I containment induced by the initial jet of the liquid inside the partially submerged downcomer

The strainers of the low-pressure ECCS system at the typical Mark II NPP are located approximately 3.63 meters (11.92 ft) below the water level. That location is almost the same elevation that the end of the downcomer pipe, as can be observed in Figure 3. The initial bubble might not reach the strainer as it form at the end of the downcomer pipe but it can reach it as the initial bubble and subsequent bubbles rise to the suppression pool surface.

On the typical Mark-III containment the ECCS strainers are located close to the outer wall of the containment pool while the horizontal vent outlets are located at the inner wall of the containment pool. The distance between the end of the vents and the strainer in the typical Mark III containment is approximately 6.7 meters. For Mark III plants it is not expected that the initial gas bubble would reach the strainers.

Figures 6, present the different locations and distance in typical BWR suppression pools.

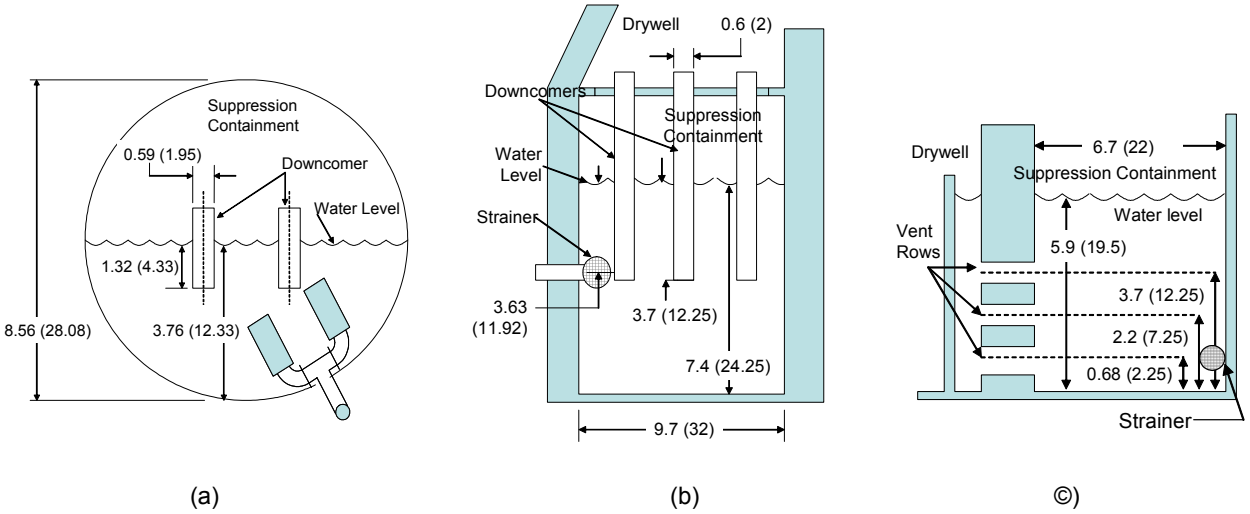

Figure 6: Typical strainer location at suppression pools of (a) Mark-I, (b) Mark-II, (c) Mark-III.

5.3 Kinetic energy injected in a Mark-I and Mark-II containment

The initial recirculation motion (vortex) in the suppression pool is caused by the injection of the column of water present in the submerged downcomer. After downcomers are clear, the upward motion of gas will combine with the initial motion of the water jet. This two forces will create a turbulent flow inside of the suppression pool. The general dynamics of the suppression pool water are very difficult to analyze. The existing numerical tools to analyze two-phase flows are not completely validated. Experimental analysis are necessary to understand the general dynamics in the suppression pool and the interaction between the gas and liquid phases.

Regardless the complexity of the pool dynamics, we can estimate the kinetic energy (KE) introduced by the column of water injected at high velocity into the suppression pool. Using equation-8, we estimated the kinetic-energy introduced in Mark-I and Mark-II containment. Table-13 presents the mass of liquid injected, according to the submergence and diameter of a single downcomer. Table-13 also summarizes the results of the impulse calculation.

$$KE = \frac{m \cdot V^2}{2} \qquad \text{Equation-8}$$

-
Where:

m = mass; and
V = velocity.

Table 13. Kinetic-energy (KJ) estimated for a single downcomer in a typical Mark-I and II containment

		Mark-I	Mark-II
number of dow mcomers		80	83
single dow ncomer area (m^2)		0.280	0.274
mass in the submerged dow ncomer (Kg)		369.43	1021.63
LOCA Category			
Category	coolant volumetric flow (m^3/s)		
1	0.00631	0.00	0.01
2	0.09465	0.57	1.65
3	0.3155	6.31	18.37
4	1.5775	157.75	459.18
5	6.31	2524.07	7346.91
6	31.55	63101.72	183672.65
Plant Specific DBA			
	2.85	514.91	1498.77

As we can observed in Table-13, the kinetic energy in Mark-II is almost 3 times higher than the kinetic-energy in Mark-I. From Table-2 we know that the volume of water in Mark-II is only 1.3 times higher than Mark-I, which means that the energy, per volume of water, injected in Mark-II containment, is more than twice than the energy injected in Mark-I.

5.4 Duration of the liquid-gas jet

To estimate the duration of non-condensable gas injection, it is assumed that the concentration of non-condensable gases in the liquid-gas jet decreases linearly until all the non-condensable gas is purged from the dry-well. Equation-9 is used to estimate the duration of the blow-down of non-condensable gases into the suppression pool .

$$dt = \frac{2 \cdot V_{drywell}}{\dot{V}_{\exp anded\ volumetric\ flow}} \qquad \text{Equation-9}$$

This calculation assumes that the expanded volumetric flow remains constant during the blow-down and that pressure and temperature at dry-well remains constant. Table-14 summarizes the estimated blow-down durations for the selected plants.

Table 14: Estimated blow-down duration of non-condensable gases (seconds)

LOCA Category	coolant volumetric flow (m^3/s)	Mark-I .	Mark-II	Mark-III
1	0.00631	3165.14	5059.49	2529.01
2	0.09465	211.01	337.30	168.60
3	0.3155	63.30	101.19	50.58
4	1.5775	12.66	20.24	10.12
5	6.31	3.17	5.06	2.53
6	31.55	0.63	1.01	0.51
Plant Specific DBA				
	2.85	7.01	11.20	N/A
	2.05	N/A	N/A	7.78

As seen from the table, to a first approximation a double-ended guillotine break (Category 6 LOCA) results in all the non-condensable gas in the dry-well being purged from the dry-well and passed to the suppression pool in less than 15 seconds regardless of the containment type. For a Category 4 LOCA, the dry-well takes about 25 seconds to be purged at a typical Mark II containment NPP.

6. ECCS STRAINERS

In response to NRC Bulletin 96-3 [Ref. 14], BWR licensees replaced the ECCS strainers to minimize their potential to become clogged with debris generated during a LOCA event. In Mark I and Mark II containment, the new strainers have a cylindrical geometry (similar to the original strainers), but have a larger surface area. Figure-7 shows a prototypical cylindrical General Electric (GE) stacked disk strainer. Some BWR licensees with Mark III containment installed a different type of strainer with a toroidal geometry.

Figure 7: Prototypical GE Stacked Disk Strainer (NEDC-32721P-A)

Figure-8 characterizes the strainer types by supplier. Suppliers of cylindrical strainers include General Electric (GE), Performance Contracting Inc. (PCI), and Asea Brown Boveri (ABB). The supplier of the toroidal strainer is Enercon Services. More than 90 percent of the Nation's BWR NPPs installed cylindrical strainers in their suppression containment.

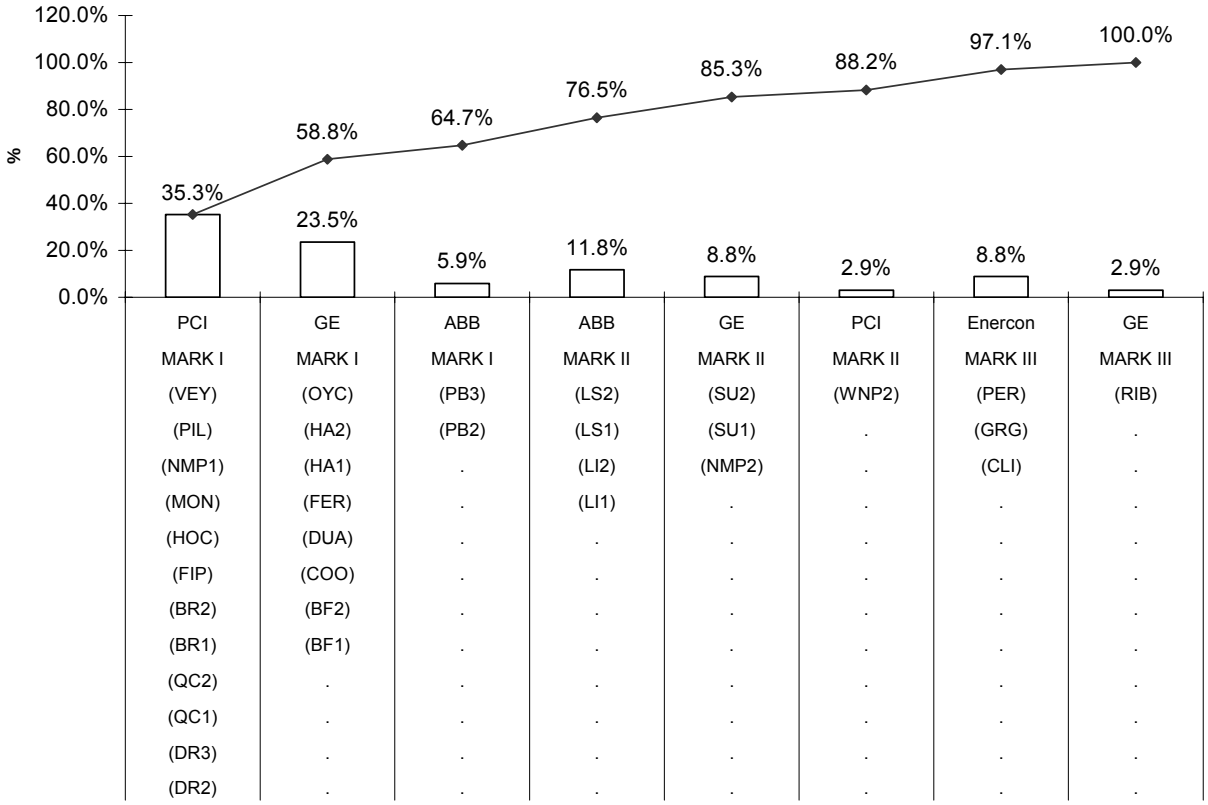

Figure 8: BWR NPP Containment-Strainer CombinationT

The typical Mark-I suppression containments used in this analysis have cylindrical strainers with a diameter of 0.9 meters (36 inches) and a hydraulic-length of 1.19 meters (47 inches), with 51,150 holes per square-meter (33 holes per square-inch). The strainer holes are 3.175 millimeter (0.125 inches) diameter.

7. ECCS SUCTION FORCE

The suction force at the ECCS strainers is the final mechanism evaluated in this report. This force is induced by ECCS pump suction flow. ECCS pump suction flow occurs in response to a LOCA ECCS actuation. The pump suction flow rate during the initial response to a LOCA varies over time due to the range of accident conditions.

Although the various types of BWRs have different geometrical characteristics, their respective ECCS components and operational response to manage a LOCA event are similar. The next two sections describe the typical ECCS components and the general response of the ECCS to a LOCA event.

7.1 ECCS Systems and Components

The ECCS is composed of two high-pressure systems and two low-pressure systems. Specifically, the high-pressure systems are the High-Pressure Coolant Injection (HPCI) system and the Automatic Depressurization System (ADS). The low-pressure systems are the Low-Pressure Coolant Injection (LPCI) mode of the Residual Heat Removal (RHR) system and the Low Pressure Core Spray (LPCS) system [Ref. 15].

The HPCI system provides emergency core coolant to maintain reactor coolant inventory for small-break LOCAs. If the HPCI system is not adequate, the ADS depressurizes the reactor down to a pressure where the LPCI and LPCS systems can provide emergency core coolant to maintain reactor coolant inventory in the reactor vessel. The LPCS system provides spray cooling above the core to mitigate the consequences of a large-break LOCA, and the LPCI injects coolant to mitigate the consequences of a large-break LOCA by reflooding the core from below in order to restore and maintain adequate coolant height within the reactor core.

The ECCS low pressure systems are initiated by either a “low-low” (level 1) reactor water level or a high dry-well pressure coincident with “low” (level 2) reactor water level. The initiation set-point of “low” reactor water level is low enough to allow the HPCI system to return the water level to normal operation for small breaks without unnecessarily initiating the ADS. By contrast, the low-low reactor water level (level 1) is high enough to allow the low-pressure system to start with enough time to avoid the cladding temperature reaching the design-basis maximum temperature. High dry-well pressure initiates both the high- and low-pressure systems at their minimum flows. The reactor water level dictates which of the systems is adequate to return the reactor water inventory to a secure level.

As soon the ECCS receives the initiation signal, a recirculation flow path is established between the ECCS pumps and the suppression pool. This recirculation path allows the minimum flow required to avoid overheating of the pumps before it supplies water to the reactor vessel at its full capacity. The response of the ECCS to a LOCA event is automatic for 20 minutes, which is considered sufficient time for plant operators to make an operational decision. Figure 9 presents a general configuration of a ECCS system in a typical Mark-I. Based on this figure the RHR and CS pumps have a dedicated pipe line connected to one of the penetration at the bottom of the suppression containment. In addition, each RHR pump penetration has two strainers connected to the pipe by a tee and a spool piece, while each CS pump penetration has only one strainer.

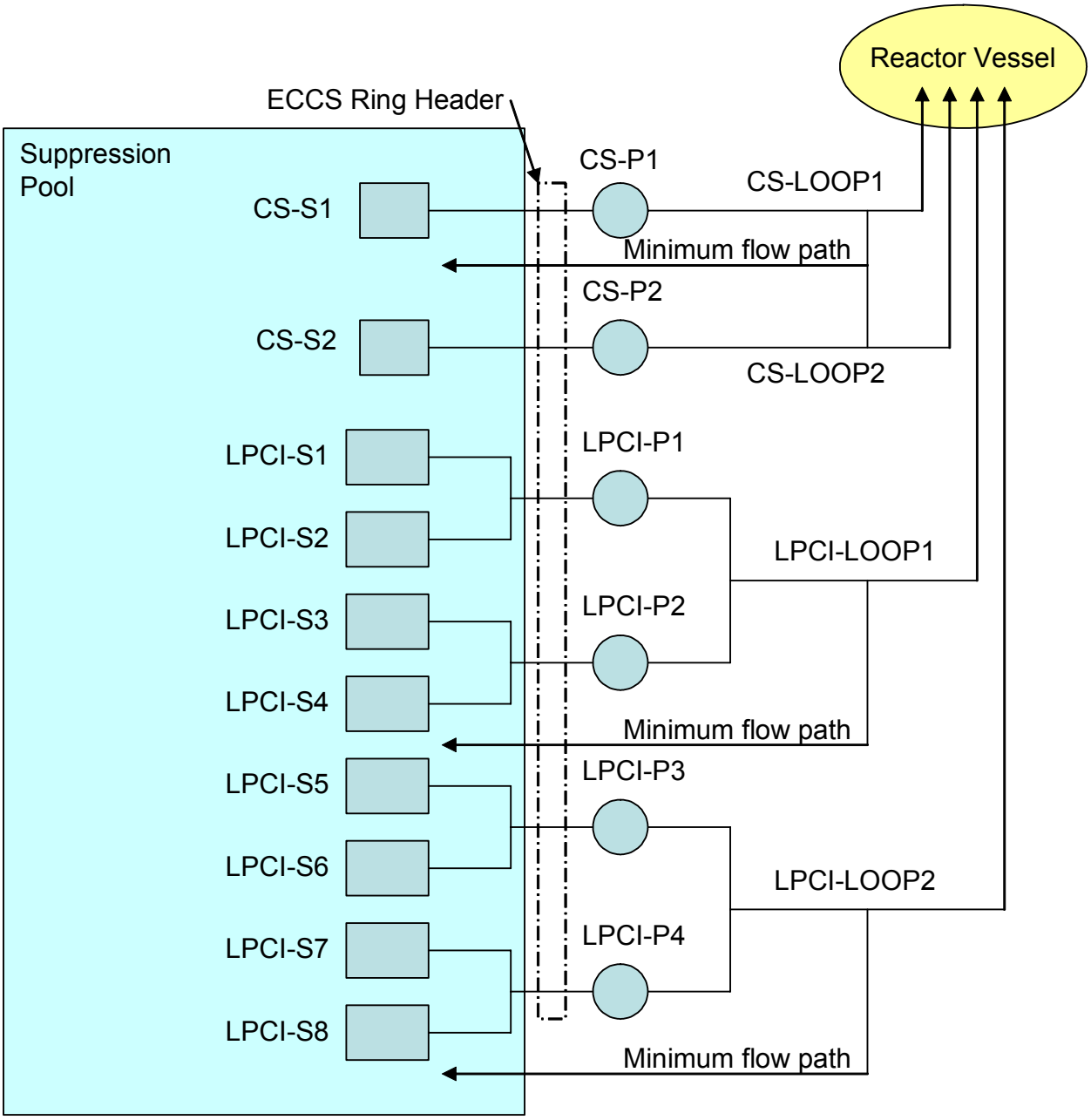

Figure 9: General BR ECCS Configuration for a typical Mark-I containment.

7.2 ECCS Responses to a LOCA Event

The HPCI system activates at minimum flow in response to either water reactor level 2 or high dry-well pressure. The HPCI pump is turbine-driven and normally aligned to draw water from the condensate storage tank (CST). However, if the water level in the CST falls below a preselected point, the suction path of the HPCI system switches to the suppression pool.

The HPCI system is designed to supply the design flow rate within 50 seconds after receiving the initiation signal, and the minimum flow develops during the first 10 seconds. After 10 seconds, the pump discharge valve and turbine steam supply valve continue to open until design flow is reached (before 50 seconds after receiving the initiation signal).

The cold water injection decreases the temperature of the reactor water, and the pressure and break leakage also eventually decrease. If the break is small, the HPCI system will be adequate to restore the reactor water level. However, if the break is of a medium or large size, the HPCI system will not be adequate, and the reactor water level will continue to decrease until it reaches level 1. At water level 1, the low-pressure system initiates at minimum flow if it has not already been initiated by high dry-well pressure.

The ADS initiates when the reactor reaches water level 1 and high dry-well pressure. In so doing, the ADS decreases the reactor vessel pressure to a point where the low-pressure system can inject water into the reactor. In the event that the reactor reaches water level 1 but not high dry-well pressure, the ADS will initiate after 13 minutes of sustained reactor water level 1.

The difference between the ECCS responses to medium and large-sized LOCAs lies in how fast the reactor reaches water level 1. Obviously, the larger the pipe break, the faster the reactor reaches water level 1 and the sooner the low-pressure ECCS system initiates. The stroke-time of the injection valves are among the components that determine how fast the ECCS draws water from the suppression pool at its full capacity. Table 15 summarizes some operational characteristics of the low pressure ECCS.

Table 15: Typical BWR Mark I, II, and III operational characteristics

		Mark-I	Mark-II	Mark-III
CS	Number of pumps	2	2	2
	Design Volumetric Flow per pump	0.25 m^3/s @ dP 779.1 KPa	0.31 m^3/s @ dP 723.9 KPa	0.28 @ dP 779.1 KPa
	Permissible Pressure Difference (vessel-dry well)	1958.11	1992.58	1813.32
LPCI	Number of pumps	4	4	4
	Design Volumetric Flow per pump	0.61 m^3/s @ dP 137.9 kPa	0.50 m^3/s @ dP 137.9 kPa	0.28 m^3/s @ dP 137.9 kPa
	Permissible Pressure Difference (vessel-dry well)	1427.2 kPa	2033.9 kPa	1530.6 kPa

CS	Number of pumps	2	2	2
	Design Volumetric Flow per pump	4000 gpm @ 113 psid	5000 gpm @ 105 psid	4410 gpm @ 113 psid
	Permissible Pressure Difference (vessel-dry well)	284 psid	289 psid	263 psid
LPCI	Number of pumps	4	4	4
	Design Volumetric Flow per pump	9600 gpm @ 20 psid	8000 gpm @ 20 psid	4470 gpm @ 20 psid
	Permissible Pressure Difference (vessel-dry well)	207 psid	295 psid	222 psid

If normal AC power is available the two CS pumps and four LPCI pumps start immediately after receiving the initiation signal without delay. By contrast, if normal AC power is not available, the CS pumps and LPCI pump start alternatively after standby power system is ready for loading. The standby power system at the typical Mark-I used in this ananlysis is ready for loading at 12 sec.

The licensees, of the plants mentioned in the previous section have performed analysis of the ECCS response to a design basis accident (recirculation pipe double guillotine break). This analysis was done for the case when all the ECCS components and off-site power were available. General results of the sequence of the accident documented in the UFSARs, are summarized in Table 16.

Table 16: General DBA sequence (seconds)

	Mark-I	Mark-II	Mark-III
Vents clear	0.25	0.733	1st/2nd/3rd row 1.0/1.33/1.72
ECCS injection initiation	30	30	HP/LPCI/LPCS 27/37/40
End of blowdown	31.6	36.35	300

The injection of water to the reactor by the ECCS system begins whenever the permissible pressure is reached. The permissible pressure signal opens the injection valves of the ECCS system. The full capacity of the pumps is reached when the valves are fully open. The volumetric flow will depends of the pump performance criteria.

The high dry-well signal will initiate the ECCS system at minimum recirculation mode within the first seconds after the pipe break. This occurs before the permissible pressure to inject is reached. The minimum flow is established to avoid overheating of the pumps before the permissible reactor pressure send the signal to the injection valves to open. The flow during the minimum recirculation mode will depends of the pump manufacturing characteristics and plant specific procedures.

The injection of water to the reactor by the ECCS system begins whenever the permissible pressure is reached. The permissible pressure signal opens the injection valves of the ECCS system. The full capacity of the pumps is reached when the valves are fully open. The volumetric flow will depends of the pump performance criteria.

As can be observed in Table 14, the ECCS system start to inject just before the blow-downs end but almost 15 seconds after the injection of non-condensable gases, according to the previous calculations. The suction force at the strainer will start to increase and the potential of gas ingress will increase. The gas-bubbles with the higher potential to ingress into the ECCS system are the ones with the smallest diameter and the higher likely hood of been trap in the recirculation motion created by the blow-down. The other potential source of gases that may ingress, is the remaining gas injected at the end of the blow-down, which may reach the strainer. The following two sections describe a more detail analysis of the ECCS response and the influence that the ring header may have in the ECCS strainer suction force.

7.3 ECCS Strainer Average Velocity Without a Ring Header

The average velocity at the strainer is a form to characterize the suction force at the strainer. The average velocity is calculated: dividing the volumetric flow by the suction pipe nominal area. For the typical Mark-I NPP, the two nominal diameter used to calculated the area are: 0.508 meters (20 inches) and 0.609 meters (24 inches) for the CS and LPCI suction pipe respectively [Ref. 4].

The calculations presented in this section are based on information for the typical Mark-I , as summarized in Table 15. The ECCS system logic is designed to handle several scenarios, including the absence of normal AC power and failure of a single component. The average velocity in this section at the ECCS strainers is calculated for (1) no single component failure, (2) normal AC power available, and (3) a design-basis accident (DBA).

If normal AC power is available for the typical Mark-I , the two CS pumps and four LPCI pumps start immediately without delay. By contrast, if normal AC power is not available, the two CS pumps and one LPCI pump start immediately after standby power becomes available, and the other three LPCI pumps start after a 12-second delay. The standby power system for the typical BWR Mark-I is ready for loading at 12 seconds.) For both CS pumps combined, the minimum flow is around

700 gpm, while the minimum flow for two LPCI pumps combined varies from 700 to 2,500 gpm [Ref. 6].

The CS injection valves receive the permissible pressure signal and immediately begin to open 22 seconds after the pipe breaks. The valves are fully open after 10 seconds, and the flow is assumed to increase linearly from minimum (375 gpm per pump before the permissible pressure signal is received) to full capacity. Each CS pump is operating at full capacity, delivering 4,000 gpm, 32 seconds after the pipe breaks.

By contrast, the LPCI injection valves receive the permissible pressure signal 27 seconds after the pipe breaks. The valves are fully open after 51 seconds, and the flow is assumed to increase linearly from minimum (1,250 gpm per pump before the permissible pressure signal is received) to full capacity. Each LPCI pump is operating at full capacity, delivering 9,600 gpm, 78 seconds after the pipe breaks.

Table 17 summarize the evolution of the ECCS volumetric flow, assuming that minimum-flow valves open almost instantaneously, allowing 700 gpm for the two CS pumps and 2,500 gpm for the two LPCI pumps.

Table 17: Typical Mark-I NPP, Design-Basis LOCA ECCS Pump Flows for Normal AC Power and No Failures

		Flow per pump					
	Time	CS Flow (m^3/s)	LPCI Flow (m^3/s)	CS Flow (gpm)	LPCI Flow (gpm)	Total Flow (m^3/s)	Total Flow (gpm)
high dry-well pressure or reactor water level 1 signal	0	0.0237	0.0789	375	1250	0.3628	5750
285 psid permissible reactor pressure for CS	22	0.0237	0.0789	375	1250	0.3628	5750
208 psid permissible reactor pressure for LPCI	27	0.1380	0.0789	2188	1250	0.5916	9375
CS full open valve after 10 seconds	32	0.2524	0.1305	4000	2069	1.0269	16275
LPCI full open valve after 51 seconds	78	0.2524	0.6058	4000	9600	2.9278	46400

Note: The volumetric flows in the CS and LPCI columns are per pump.
The total flow was calculated for two CS pumps and four LPCI pumps.

Dividing the volumetric flow by the calculated nominal area we obtained the average flow velocity for the case where no rin header is present. Table 18 presents the evolution of this velocity. The next subsection presents the assumptions and calculations for average velocity with a ring header.

Table 18. Average Velocity at Strainer Section Pipe Without a Ring Header at a typical Mark-I

	Time	CS m/s	LPCI m/s	CS ft/s	LPCI ft/s
high dry-well pressure or reactor water level 1 signal	0	0.116728	0.135102	0.382965	0.443247
285 psid permissible reactor pressure for CS	22	0.116728	0.135102	0.382965	0.443247
208 psid permissible reactor pressure for LPCI	27	0.680912	0.135102	2.233962	0.443247
CS full open valve after 10 seconds	32	1.245096	0.22358	4.08496	0.73353
LPCI full open valve after 51 seconds	78	1.245096	1.03758	4.08496	3.404133

7.4 ECCS Strainer Average Velocity With a Ring Header

Some BWRs have a common ring header pipe outside the ECCS suppression containment, which connects all ECCS strainers and pumps and affects the average velocity at the strainers. During the first minutes of a large-break LOCA, all of the low-pressure systems draw water from the suppression pool. To simplify the calculations of average velocity at the ECCS strainers, this section draws an analogy between a pipe system and an electric circuit.

In a BWR equipped with a ring header, the 10 ECCS strainers are connected in parallel to a single header node. Using the electric circuit analogy (Kirchhoff's Law), and assuming that minor losses are negligible, the pressure decrease is the same at each strainer [Ref. 16]. With this assumption, the Bernoulli equation reduces to the kinetic energy term [Ref. 17], which is then used to calculate the pressure decrease caused by flow acceleration from zero velocity at the suppression pool to the average velocity inside the ECCS penetration pipe (Equation 10).

$$\Delta P = \frac{\rho V^2}{2}$$ Equation 10

Where:

ΔP = pressure drop from zero velocity to the average velocity inside the ECCS pipe,
ρ = water density, and
V = fluid velocity.

The average velocity inside the pipe network is defined by the nominal area of the suction pipes. If the pressure decreases, it decreases at each of the 10 strainers and Equation-10 simplifies to the following equation, which can be expressed in terms of volumetric flow.

$$V_{LPCI}^2 = V_{CS}^2$$

$$\left(\frac{\dot{V}_{CS}}{A_{CS}}\right)^2 = \left(\frac{\dot{V}_{LPCI}}{A_{LPCI}}\right)^2$$

Where:

$\dot{V}_{CS}$ = volumetric flow of the CS suction pipe,

$\dot{V}_{LPCI}$ = volumetric flow of the LPCI suction pipe,

A_{CS} = cross-sectional area of the CS suction pipe, and

A_{LPCI} = cross-sectional area of the LPCI suction pipe.

Substituting this expression in the mass conservation equation, assuming incompressible flow for this system, we obtain the average velocity at the ECCS strainers (Equation 11).

$$\dot{V}_{TOTAL} = 2 \cdot \dot{V}_{CS} + 8 \cdot \dot{V}_{LPCI} \qquad \text{Equation-11}$$

Table-19 summarizes the results of the calculations for the average velocity at the CS and LPCI system with ring-header.

Table 19: Average velocity at strainer Section pipe with a ring header for a typical Mark-I NPP.

	Time	CS-RH m/s	LPCI-RH m/s	CS-RH ft/s	LPCI ft/s
high dry-well pressure or reactor water level 1 signal	0	0.110622	0.136162	0.362933	0.446724
285 psid permissible reactor pressure for CS	22	0.110622	0.136162	0.362933	0.446724
208 psid permissible reactor pressure for LPCI	27	0.180362	0.222003	0.591739	0.728355
CS full open valve after 10 seconds	32	0.313099	0.385385	1.027229	1.264386
LPCI full open valve after 51 seconds	78	0.892672	1.098764	2.928715	3.60487

As illustrated in Figure-10, the average velocity at the two CS pump strainers *decreases* 37% with the presence of a ring header, while the average velocity at the eight LPCI strainers *increases* 28% with the presence of a ring header.

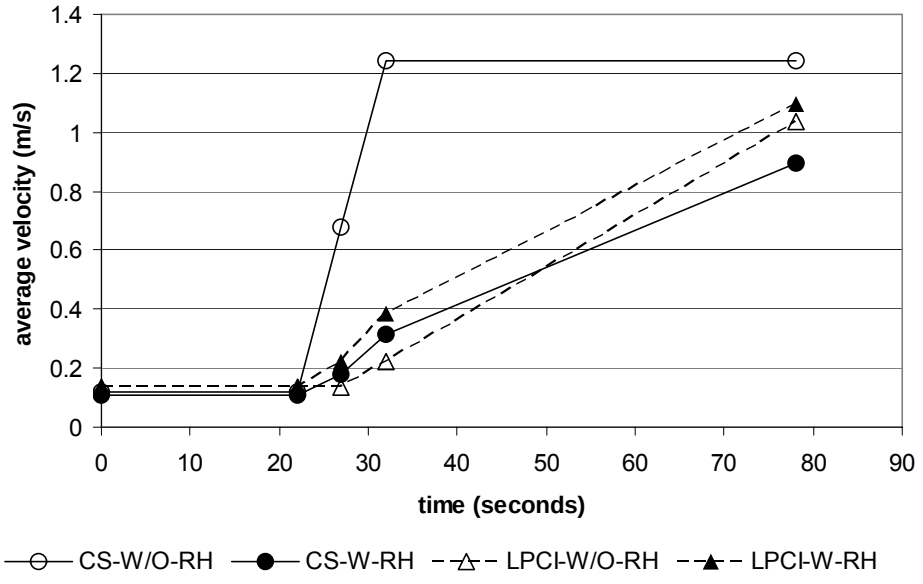

Figure 10. Average Velocity at Strainers in a typical Mark-I NPP
During Design-Basis LOCA Event With (W-RH) and Without a Ring Header (W/O-RH).

This velocity can be used to analyze the flow field to which gas bubbles in the suppression pool are exposed and the potential to be drawn by the ECCS suction force. The next section presents the summary of this report.

8. SUMMARY

GEOMETRICAL

NON-CONDENSABLE GAS SOURCES

The principal source of non-condensable gases that may enter into the ECCS system is the gas from the drywell. The amount of gas that may enter into the ECCS system depends of the free volume of the dry well and thermodynamics conditions of the gas inside the drywell at the moment of the HELB.

The amount of non-condensable dissolved in the suppression pool, represent no more than 2% of void fraction. Nevertheless is was incorporated in this analyses, due to the low sensibility of centrifugal pumps to low percent of void fractions.

MECHANISM THAT MAY CAUSE GAS INGRESS

The blowdown force and the ECCS suction force have been identified as the two driven forces of the suppression pool dynamics during HELB. The blow down force generates four potential mechanism of gas ingress: (1) the liquid-gas jet, (2) pool temperature and (3) pressure change, and (4) the turbulence. The ECCS suction has the potential to drawn gas from the suppression pool and cause a pressure drop at the ECCS strainer, causing gas coming out of the water.

The column of water of the partially submerged downcomer generates an initial liquid jet, which kinetic energy has been identified as a major force to break bubbles and to generate a circular motion (vortex) in the suppression pool. Among the three containment analyzed in this report, the column of water of Mark-II, was found to have the higher kinetic energy.

In Mark-I and Mark-II, the downcomers areas are similar and the water, in the suppression pool, is at similar temperature. For that reason the kinetic energy is proportional the submergence depth of the downcomer.

The recirculation induce by the liquid and gas jets (vortex) has the potential to keep gas bubbles in the suppression pool water, increasing the potential of gas ingress when the ECCS pumps start to drawn water from the suppression pool.

DOWNCOMERS

This technical assessment of GSI-193 has identified the alignment between the downcomer and ECCS strainers in BWR Mark I containment as the most significant geometrical characteristic that may cause gas ingress in the ECCS during the initial blowdown of a LOCA event.
This is because the alignment may cause the gas-liquid jet to reach the ECCS strainers.
Notably, nearly 65 percent of all BWR NPPs in the United States have Mark I containment with cylindrical strainers.

By contrast, the downcomer and strainers in Mark II containment are not aligned to exacerbate gas ingress during the initial blowdown. Nonetheless, the strainers' suction flanges are aligned in the path of the natural upward motion of the rising bubbles, and this will expose the strainers to gas bubbles during the blow down process.

OPERATIONAL

ECCS OPERATION

The operation of the ECCS system with normal AC power and without failure of any ECCS component is the operational status that may cause the greatest ingress of gas into the system. This status is the fastest to start the flow of suppression pool water into the ECCS (immediately upon the start of a LOCA event), and it is characterized by the highest volumetric flow.

RING HEADER

Without the presence of a common header in the ECCS pipe of the BWR Mark I NPP analyzed in this report, the average velocity at the CS pump strainer increases more rapidly than the average velocity at the LPCI pump strainer. By contrast, a ring header decreases the average velocity at the two CS pump strainers, but increases the average velocity at the eight LPCI pump strainers. Thus, the presence of a ring header deters gas ingress through the two CS pump strainers, but exacerbates it through the eight LPCI pump strainers.

REFERENCES

[1] Memorandum from F. Eltawila to C. Paperiello, Task Action Plan for resolving generic safety issue 193, "BWR ECCS suction concerns," dated May 24, 2004.

[2] Title 10, Section 50.46(b)(5), of the *Code of Federal Regulations* (10 CFR 50.46)

[3] Office of the Secretary of the Commission (SECY-04-0060) document from W.D. Travers to The Commissioners, Loss-of-Coolant Accident break frequencies for the option III risk-informed reevaluation of 10 CFR 50.46, Appendix K to 10 CFR Part 50, and general design criteria (GDC) 35, dated April 13, 2004.

[4] Final Safety Analysis Report for a typical BWR Mark-I NPP

[5] Final Safety Analysis Report for a typical BWR Mark-II NPP

[6] Final Safety Analysis Report for a typical BWR Mark-III NPP

[7] Wark, K., "*Advanced Thermodynamics for Engineers*," MacGraw-Hill, Inc., 1995.

[8] Gerrard, W., "*Solubility of gases and liquids," Plenum Press*, 1976.

[9] Baranenko, V. I., Sysoev, V. S., Fal'kovskii, L.N., Kirov, V. S., Piontkovskii, and Musienko, A. N., "The solubility of Nitrogen in Water," Atomaya Energiya, Vol 68, No. 2, pp. 133-135, August 19, 1988.

[10] Memorandum from S. Rubin to C. Michelson, Engineering evaluation - Potential for air binding or degraded performance of BWR RHR system pumps during the recirculation phase of a LOCA, dated March 31 1982.

[11] Wallis, G. B., "One-dimensional two-phase flow," MacGzraw Hill, 1969

[12] Perry, R. H., " Perry's chemical engineers' handbook, 5th edition" McGraww Hill 1973

[13] Panton, R. L. , " Incompressible flow 2nd edition," John Wiley & Sons, Inc., 1996.

[14] NRC Bulletin 96-03, "Potential Plugging of Emergency Core Cooling Suction Strainers by Debris in Boiling-Water Reactors," U.S. Nuclear Regulatory Commission, Washington, DC, May 1996.

[15] "System Manual General Electric Technology," Volume I, Revision 0197, U.S. Nuclear Regulatory Commission, Washington, DC, January 1997.

[16] Budak, A., *Circuit Theory Fundamentals and Applications*, Prentice-Hall, Inc., Upper Saddle River, New Jersey, 1978.

[17] Panton, R.L., *Incompressible Flow*, 2nd Edition, John Wiley & Sons, Inc., Hoboken, New Jersey, 1996.